The Polar Oceans Program of the Alaska SAR Facility

W.F. WEEKS,[1] G. WELLER[1] and F.D. CARSEY[2]

ABSTRACT. The science plan for the Alaska SAR Facility (ASF) focuses on earth surface characteristics that are of interest within the overall concept of global change and that show significant regional, seasonal and interannual variations resulting in changes in the strength of their radar returns. The polar oceans, with the continuous motion and deformation of the pack ice and the changes in the surface state of the surrounding open seas, offer excellent opportunities for such research. Because such studies require both frequent and detailed analysis of Synthetic Aperture Radar (SAR) data, a Geophysical Processor System (GPS) has been developed to speed the extraction of useful geophysical information from SAR data sets. This system will initially produce three main types of products: a) sets of ice motion vectors obtained by automated computer tracking of identifiable ice floes on sequential images, b) the areal extent and location of several different ice types and open water and c) a characterization of the wave state in ice-free regions as well as within the ice in the marginal ice zone at locations where significant wave penetration occurs. Details of these analysis procedures are described. Initially the GPS is planned to process 10 image pairs/day for ice motion, 20 images/day for ice type variations and 1 image/day for wave information, with a total estimated processing time of 13 hours. A variety of projects plan to utilize the SAR data stream in studies of ice, lead and polynya dynamics and thermodynamics. A common feature of these research programs will be attempts to provide, via the coupling of the SAR data with ice property and ice dynamics models, improved estimates of the heat and mass fluxes into both the atmosphere and the ocean as affected by the characteristics of the ice cover.

Key words: SAR, radar, sea ice, image analysis, remote sensing

RÉSUMÉ. Le projet scientifique aux installations alaskiennes de radar à antenne synthétique (ASF) porte sur les caractéristiques de la surface terrestre qui présentent un intérêt dans le contexte général des changements à l'échelle planétaire et qui révèlent d'importantes variations régionales, saisonnières et interannuelles aboutissant à des changements dans l'intensité des échos de radars. Les océans polaires, avec le mouvement et la déformation continue de la banquise et les changements dans l'état de la surface des eaux libres avoisinantes, se prêtent bien à ce genre de recherche. De telles études nécessitant des analyses fréquentes et détaillées des données du radar à antenne synthétique (RAAS), un processeur de données géophysiques a été mis au point pour accélérer l'extraction de l'information géophysique utile à partir des ensembles de données du RAAS. Ce système va fournir pour commencer trois sortes principales de produits: a) des ensembles de vecteurs de déplacement de la glace obtenus par le suivi automatique à l'ordinateur sur des images séquentielles de floes identifiables; b) la superficie et l'emplacement de plusieurs sortes de glace et d'eau libre et c) un schéma de l'état de la vague dans les zones libres de glace ainsi qu'à l'intérieur des glaces dans la zone marginale, à des sites où se produit une importante pénétration des vagues. On fournit des détails sur ces procédures d'analyse. On a prévu qu'au début, le processeur de données traiterait quotidiennement 10 paires d'images pour le mouvement de la glace, 20 images pour les variations du type de glace et 1 image pour le comportement des vagues, avec une durée totale de traitement estimée à 13 heures. Divers projets prévoient d'utiliser les données du RAAS transmises en continu, dans l'étude de la dynamique et de la thermodynamique de la glace, des chenaux et des polynias. Un trait commun de ces programmes de recherche sera d'essayer de fournir, par le biais du jumelage des données du RAAS avec des modèles des propriétés de la glace et de sa dynamique, de meilleures estimations des flux de chaleur et de masse à la fois dans l'atmosphère et dans l'océan, en tenant compte de la façon dont ces flux sont affectés par les caractéristiques de la couverture de glace.

Mots clés: RAAS, radar, glace de mer, analyse d'images, télédétection

Traduit pour le journal par Nésida Loyer.

INTRODUCTION

The potential of satellite-borne Synthetic Aperture Radar (SAR) for providing useful all-weather observations of both the open ocean and its ice cover was clearly demonstrated in 1978 by Seasat during its 4-month lifetime (Hall and Rothrock, 1981; Leberl et al., 1983; Napolitano et al., 1989). The development of the Alaska SAR Facility (ASF) is the result of the realization by the National Aeronautics and Space Agency (NASA) that a SAR-receiving station in Alaska would greatly expand the spatial coverage possible from the European Space Agency's ERS-1 satellite. This satellite, which does not carry a tape recorder, must be within the line of sight of the receiving station while the on-board SAR system views the area of interest on the Earth's surface. For ERS-1 the primary initial area of interest for SAR coverage is the Arctic, a region where this sensor has impressive observational capabilities. Therefore we will focus on the Arctic in our discussion. Later, ASF will also obtain SAR data from the Japanese satellite J-ERS-1 (launch 1992), as well as from the Canadian Radarsat (launch 1994). These latter satellites will carry tape recorders, thereby allowing ASF to down-link data acquired from the Antarctic. In fact, the three combined missions will provide an essentially continuous set of SAR observations, and at some times multisatellite multifrequency observations, from 1991 until 1999. From NASA's perspective, an additional important consideration leading to the establishment of ASF was the realization that the learning experience gained through the operation of the station could serve as a developmental ramp leading to the deployment of a SAR system in the late 1990s as part of NASA's Eos program.

Satellite studies of the behavior of the world's sea ice covers are particularly important because sea ice, with its associated snow cover, serves as an insulative layer separating the frigid arctic atmosphere from the comparatively warm underlying ocean. In fact, heat fluxes through typical thick multiyear ice are two orders of magnitude less than fluxes observed under equivalent meteorological conditions through newly formed ice-free leads (Badgley, 1966). The presence of a sea ice cover also changes the surface albedo of the sea from a value of 0.15 (open water) to 0.84 (dry snow on the surface of the sea ice). Therefore decreases in sea ice extent and thickness caused by a climatic warming would result in a pronounced positive feedback amplifying the observed change. Simply put, a warming trend would be expected to result in

[1]Alaska SAR Facility, Geophysical Institute, University of Alaska Fairbanks, Fairbanks, Alaska 99775-0800, U.S.A.
[2]Jet Propulsion Laboratory (MS-300-323), 4800 Oak Grove Drive, Pasadena, California 91103, U.S.A.

a decrease in sea ice extent and thickness, which, in turn, would cause further atmospheric and oceanic warming, resulting in even further decreases. It is this sea ice feedback that contributes significantly to the large mean annual temperature increases that have been projected for the Arctic in simulations of the global greenhouse scenario (Manabe and Stouffer, 1980). Based on such analyses, sea ice extent and thickness would appear to be sensitive indicators of climate change, resulting in considerable interest in developing procedures for monitoring the extent and behavior of this material. In such a monitoring program, both passive and active microwave techniques have important roles to play. Passive systems with resolutions in the range of tens of kilometres, broad coverage and good discrimination of ice extent are particularly suited for global monitoring. On the other hand, active systems, such as those discussed here, offer the capability of monitoring sea ice areas of critical importance in considerable detail and of exploring the mechanistic aspects of sea ice drift and deformation and ocean-atmosphere exchange.

SEA ICE AND SAR

The arctic ice pack can, in a general way, be considered to comprise two primary ice types, first year and multiyear, with the first-year ice forming during the present growth season. If this ice survives the following summer melt season, it becomes multiyear at the start of the new growth season. These two ice types are different in several important respects, with first-year ice being both more saline (4 to 15‰ vs. 0 to 4‰) and thinner (<2.5 m vs. 2.5–6 m).

The ice at a given location moves under the forces exerted upon it by the local winds and currents, as well as the stress transmitted to it through the ice pack. This latter stress is referred to as the internal ice stress and can be transferred over hundreds of kilometres. Typical pack ice velocities range from 0 to 20 cm/s, although extreme velocities of up to 4 m/s (8 knots) have been recorded. During the winter, periods of zero ice motion are not rare. During the summer, when the pack is more open, the ice appears to drift continuously, with the highest velocities invariably occurring at locations near the edge of the pack in regions where interfloe interference is minimal. Studies using recent buoy drifts, as well as the drifts of manned camps and beset ships, reveal that in the Arctic Ocean the ice pack has a very systematic mean motion, with a large clockwise gyre occurring in the Beaufort Sea to the north of Alaska and a Trans-Polar Drift Stream formed by the motion of ice from the Siberian Shelf over the Pole to exit from the basin via Fram Strait between Greenland and Svalbard (Colony and Thorndike, 1984). Although the average drift values appear consistent and well behaved, recent satellite observations show a much more complicated short-term picture; for example, the Beaufort Gyre can reverse for periods of several weeks (Serreze *et al.*, 1989).

The differential motions resulting from the drift of the ice cause the formation of two very different types of features that characterize the sea ice environment. The first of these features, leads, initiate as cracks that form during divergent periods of ice motion and open to widths varying from a few metres to a few kilometres. Lead lengths extend to tens or even to hundreds of kilometres. Leads produce open water and thin ice areas that dominate the heat flux into the atmosphere and the salt flux into the ocean. In contrast to

this are pressure ridges that form during periods of ice convergence. There appear to be two types of such features: sinuous ridges, which form when the compressive ice motions are approximately normal to the initial crack or lead, and straight shear ridges, which result from motions parallel to the initial crack or lead (Weeks *et al.*, 1971). Both ridges in general and shear ridges in particular appear to be more frequent near fixed features such as coastlines. Understanding pressure ridges is essential to understanding pack ice behavior in that ridging transfers thin ice to thick ice by a rapid mechanical process that replaces the much slower process of normal ice growth. As such, ridging controls the thick end of the ice thickness distribution, while lead formation and the ensuing growth of new ice within the leads controls the thin end of the distribution. The pattern of active leads and ridges is controlled primarily by meteorological conditions and can change quite rapidly. Although the locations of the cracks that initiate the lead and ridge process do not appear to be significantly influenced by ice thickness, once ridging starts the deformation tends to be localized in the thinner, weaker ice that recently formed in the lead systems. This is such a striking effect that some sea ice models idealize thicker multiyear ice as being undeformable.

To understand SAR returns from sea ice, one must consider the salinity of the ice. The amount of salt entrapped in sea ice is a linear function of the salinity of the sea water and a non-linear function of the growth velocity of the ice. During the growth season, in first-year ice the temperature and salinity profiles result in brine contents within the ice that characteristically range from 1 to 10‰ near the upper ice surface and 20 to 30‰ by volume near the ice-water interface. Of the two primary phases that constitute sea ice, the ice itself is a relatively low-loss dielectric with a skin depth at typical SAR frequencies of a few metres. For instance it is known that X-band side-looking airborne radar (SLAR) can penetrate lake ice with thicknesses of 2 m, providing useful information on which portions of lakes are frozen completely to the bottom (Weeks *et al.*, 1981). In a similar manner, radar pulses readily penetrate the snow cover characteristically present on top of the sea ice. This is hardly surprising in that during the ice growth season the snow cover is simply a mixture of pure ice and air. In fact, the only time when the presence of a snow cover appears to have a discernible effect on the radar return from sea ice is during the late spring and summer, when the snow cover contains free water, a very lossy material. The liquid or brine phase in sea ice is also a very high-loss dielectric with loss values similar but higher to those of sea water. Unfortunately the combinations of ice and brine that characterize first-year ice also result in a high-loss material. As a result there is little penetration of the radar pulse into such ice and the strength of the return is controlled by the roughness of the upper ice surface. A schematic diagram showing this situation is given in Figure 1. As indicated, when the return to the receiver is considered, flat, newly formed sea ice gives little return and can be confused with the return from a flat, calm sea. However, as newly formed leads are composed of either open water or thin, flat ice, they provide a readily identifiable signal. In fact, when the air temperature at the time of lead formation is considered, the open water/thin ice ambiguity commonly ceases to be a major problem.

In contrast to first-year ice, the upper portion of multiyear ice has a very low salinity as a result of a brine-flushing
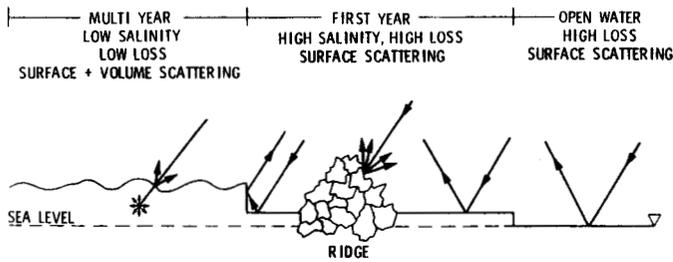
FIG. 1. Interactions between radar and different sea ice types (SIR-C, 1986). See text for explanation.

process that occurs during the melt season. The lower portion of multiyear ice is, of course, really first-year ice that formed during the present growth season. As such it is relatively salty, with an associated large brine volume. Multiyear ice is essentially a two-layer system composed of a low-loss upper layer and a high-loss lower layer. Although the radar pulse does not penetrate completely through the ice, there is significant penetration into the upper layer, where appreciable volume scattering occurs. The result is that multiyear ice has a significantly higher radar cross-section than first-year ice, allowing ready discrimination between these major ice types. Pressure ridge sails, being composed of blocks of either first-year or multiyear ice, also give strong radar returns as the block edges act as series of corner reflectors. In addition, ridges can in many cases be identified by their characteristic surface patterns. In summary, features identifiable in SAR images include individual ridges and rubble areas, leads, first-year and multiyear ice and, in most cases, open water. This latter case is particularly interesting in that, although open water can, as a function of sea state, give radar returns that are less (calm sea) or more (large waves) than any sea ice type, the combination of the strength of the return and its areal pattern usually allows for unambiguous separations between ice and water.

THE ASF OCEANS PROGRAM

Ice-Covered Oceans

Ice Circulation and Mass Balance: Presently the circulation patterns of arctic sea ice are only known on the largest of scales based on data obtained from beset ships, drift stations, buoys and satellites. SAR observations will allow the movements and deformation patterns to be examined on a wide range of scales extending down to the sizes of individual interacting ice floes. Particularly interesting will be the detailed ice motion information expected from locations near the ice edge in the southern Bering Sea, where even buoy data is limited. The temporal repeat of the sampling will usually be three days during the ERS-1 mission, with more frequent sampling possible after J-ERS-1 and Radarsat are in operation. Several problems that should be resolved by improved information on the circulation of the ice include the amount of ice production that occurs over the the arctic continental shelves, the amount of ice formed within the slowly diverging central pack and the distribution of ice types within the central pack and the marginal seas.

Heat, Mass and Momentum Fluxes: When the Arctic is considered in light of projected global changes, improved estimates of the heat, mass and momentum exchanges among the atmosphere, the ice and the ocean in the Arctic are crucial.

Although SAR cannot measure these fluxes directly, it can provide observations required for improved estimation. For instance, as described in more detail later, SAR can provide information on changes in the amounts of different ice types and on the dates of formation and areal extent of leads and pressure ridges. This information, when combined with descriptions of the local atmospheric and oceanic conditions, should produce improved estimates of the requisite surface heat fluxes as a function of ice thickness. In particular the SAR observations should offer the possibility of examining seasonal and regional variations in these fluxes.

Ice Pack Morphology and Air-Ice Ocean Momentum Transfer: The drift of pack ice is determined by the momentum balance between the wind and current forces on the upper and lower surfaces of the ice, the Coriolis force resulting from the fact that the ice is drifting on a rotating earth, and the stresses generated within the ice by ice-ice interactions. SAR will provide information that can be related to both the temporal and the spatial distribution of the roughness of the upper surface of the ice and presumably to the roughness of the lower surface. This information should prove useful in improving estimates of the appropriate drag coefficients and perhaps provide approaches leading to their remote estimation.

Rheological Descriptions of Sea Ice: Although considerable information is available on the rheological behavior of small specimens of sea ice, little is known about the most appropriate way to express constitutive laws that describe pack ice behavior. To date the stress is commonly taken to depend on both the deformation or strain rate and on the ice conditions, particularly on the amounts of open water and thin ice. ASF SAR data should provide the combination of improved ice deformation data and ice type information that will allow critical comparisons to be made of the degree to which different rheological models approximate actual pack ice behavior.

Land-Air-Sea-Ice Interactions: In near-coastal areas the presence of land influences the behavior of the pack over the continental shelves. Ice deformation in such regions is particularly intense and is influenced by factors such as drag against the coastal fast ice and by ridge keel drag along the sea floor. SAR will provide a time series of the changes in the nature of the ice cover in this zone, changes that undoubtedly can be related to the nearshore bathymetric conditions and currents. Of particular interest are the islands of grounded ice that are known to form in shoal areas of the Chukchi Sea. Observations of ice behavior around such natural features could also contribute insights useful in the design of offshore structures for such shelf regions.

Marginal Ice Zone Processes: Although recently there has been considerable interest in marginal ice zone processes (Muench et al., 1987), it has only been possible to maintain in situ field observations in such areas for short periods of time. SAR should provide an ideal tool for expanding the observational base in such regions in that it provides detailed descriptions of ice types and their geometric characteristics as well as of wave conditions at both the ice edge and for a significant distance into the pack.

Open Oceans

The ASF station mask also covers vast regions of the Chukchi and Bering seas and of the North Pacific Ocean

that are either seasonally or continually ice free (Fig. 2). As in the ice-covered areas, SAR is capable of providing useful information concerning a number of processes and ocean features.

Surface Waves: Because SAR can be used to produce the directional wave spectra of storm-generated wave fields, studies of ERS-1 data should contribute to the current understanding of the dispersion, spatial evolution and "climatology" of such fields within the station mask. Such measurements could be of appreciable value in verifying wave hindcast models and in updating forecast models. Because strong currents also occur within the station mask, information can also be gained on wave-current-wind interactions that should lead to improvements in wave now-cast and forecast capabilities.

Internal Waves: To date, imaging radar systems have primarily detected tidally generated internal soliton waves over shelf breaks and in shallow water, allowing estimates to be made of their amplitude and energy (Fu and Holt, 1983, 1984; Apel and Gonzalez, 1983). Although only the tidally generated and larger coastal internal waves are likely to be detectable using ERS-1 data, interesting studies are still possible because of the low salinity lenses of surface water, formed from sea ice melt and river discharge, that occur over the shelves of the Arctic Ocean. Similar features also occur during the summer over the Aleutian and Gulf of Alaska shelf breaks, where a sharp seasonal thermocline results from the large amounts of freshwater runoff entering the sea from the major coastal rivers. Ideal conditions for internal wave formation presumably result.

Currents, Fronts and Eddies: A variety of mesoscale circulation features, including thermal fronts, eddies and boundary currents, are known to occur in the waters within the ASF station mask. Although such features are observable through the use of infrared (IR) sensors, these systems are limited by the frequent cloud cover encountered in the North Pacific and the Arctic. In addition, studies in the Gulf of Alaska indicate that during most periods water temperatures are so uniform that infrared images commonly do not reveal circulation boundaries (Royer and Muench, 1977). However,

analysis of Seasat SAR from the Chukchi Sea indicates that frontal systems in that region are detectable as the result of slight changes in the roughness of the sea surface. If such situations prove to be generally common, SAR imagery could prove to be very useful in monitoring mesoscale circulations.

Bottom Topography: One of the surprising results of Seasat was that it was possible to locate submerged objects, such as ships in the English Channel, through the modulation of short surface gravity waves by surface currents that were changed as a result of the presence of the object. The ASF station mask offers a variety of opportunities for such investigations. Particularly interesting locations would appear to be the deltas of rivers such as the Kuskokwim, Yukon and Mackenzie, where studies over time of changes in water depths and currents would be both scientifically interesting and operationally useful.

Atmospheric Conditions: Since atmospheric conditions such as rain and variations in the wind field resulting from fronts, storms and mesoscale wind variations affect the short gravity waves that are the primary contributors to radar backscatter, variations in these conditions can be indirectly observed by SAR. Such information will be particularly useful when combined with results from other satellite sensors.

THE GEOPHYSICAL PROCESSOR SYSTEM

In cases where timeliness is of no importance, the classical procedure of providing images to interested investigators and reading the results in journals two to five years later will still suffice. However, manual procedures clearly are not sufficient if rapid results would add to the usefulness of the analysis. For instance, in the past the tracing of ice floe movements between two different SAR images could require as much as a full day in front of a computer terminal, leaving the scientist in a state of near rigor mortis by evening. Based on the Seasat experience and the fact that, soon after launch of ERS-1, ASF will be receiving and processing 20-40 images a day, traditional means of SAR data analysis clearly will not suffice if investigators hope to keep up with the data flow. Obviously scientists requiring observations on ice floe motions would have an analysis backlog by the end of the first day of data collection.

The answer to the above problem is the Geophysical Processor System (GPS), which was developed through a joint effort by the Jet Propulsion Laboratory (JPL) and the Vexcel Corporation and was installed at ASF during early 1991. The purpose of this system is to speed the routine manipulation and extraction of geophysically interesting products from the SAR images produced at the ASF by providing a series of fully automated analysis procedures. At launch the GPS will produce ice motion products from sequential SAR images, an ice classification product and smoothed and contoured ocean wave spectra.

Ice Motion Tracking: Clearly one task common to many of the science programs is keeping track of the movements of identifiable ice floes in sequential imagery and converting this information into a series of vector fields displayed on some convenient grid. As this is a repetitive and time-consuming task, it was the prime candidate for GPS implementation. For some time it has been known that a large number of ice features both within floes and along floe and lead boundaries can usually be identified on sequential radar images of sea ice and utilized to estimate ice motions
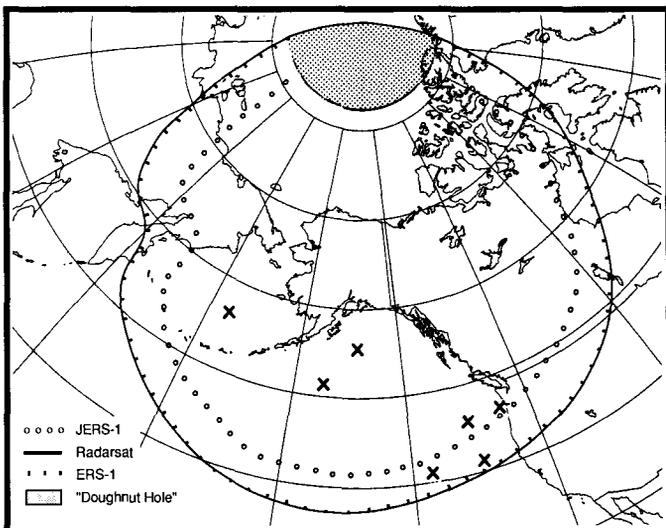

FIG. 2. The estimated ASF station mask based on signal receptions from satellites orbiting at elevations similar to that of ERS-1. The crosses indicate the locations of NOAA wave rider buoys. Note that the ERS-1 and Radarsat masks are essentially the same.

(Hall and Rothrock, 1981; Leberl *et al.*, 1983; Curlander *et al.*, 1985; Carsey and Holt, 1987).

The GPS ice motion tracking algorithm design has been described by Kwok *et al.* (1990). Key steps necessary to automate a floe-tracking procedure are (Fig. 3): 1) selection of image pairs, 2) feature extraction, 3) area or feature matching, 4) consistency checks and filtering and 5) preparation of data products.

The ice motion tracker will utilize low-resolution (100 m pixel spacing, 240 m resolution) imagery, with each image being 100 × 100 km in size. The selection of the image pair or pairs most likely to have identical ice features is made by estimating the short-term drift of the ice region of interest via the use of a linear model based on observed ice drifts that relates the mean ice velocity u to the geostrophic wind G: u = A G, where A is a seasonally dependent complex multiplier composed of a scaling factor and an ageostrophic drift angle (Thorndike and Colony, 1982). As 70% of the variance in the ice motion can be explained by the wind alone on the time scales of a few days to weeks, this procedure is expected to provide adequate motion estimates in regions well removed from coastal influences. The wind estimates required to drive this model will be based on the University Data System (Unidata) data stream, which will be received at ASF by direct satellite link. Unidata provides the results of the gridded real-time analyses of the National Meteorological Center and the European Centre for Mediumrange Weather Forecasting. In shallow water areas, such as parts of the Bering and Chukchi seas, an alternate model developed by Pease and Overland (1984) that requires bathymetric input
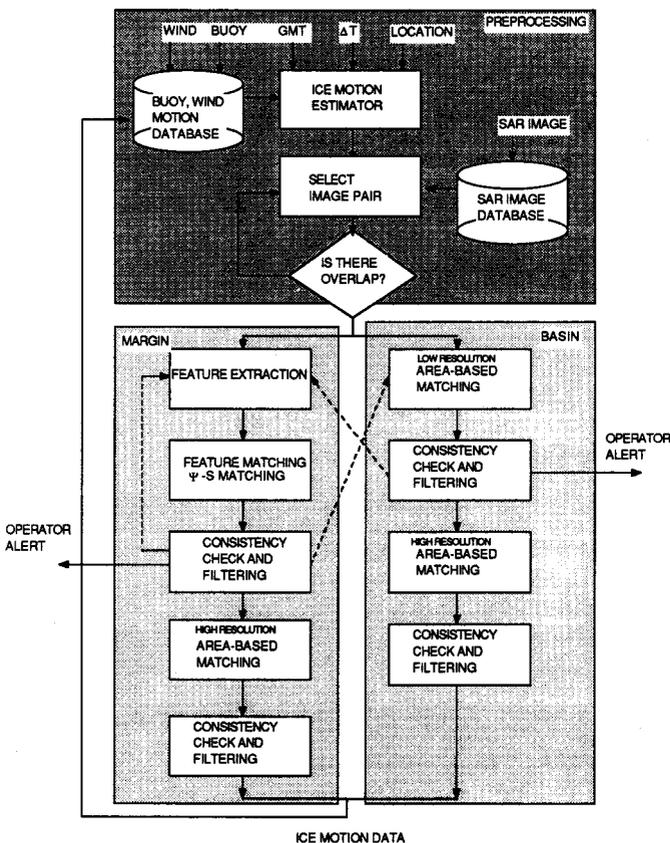

FIG. 3. Diagram outlining the flow of the feature-based and area-based algorithms used in the ice motion tracking program. (Reprinted with permission from Kwok *et al.*, 1990 ©1990 IEEE.)

may also prove to be useful. In the worst case an exhaustive feature search could be carried out until matching features are found. However, this procedure could require undue amounts of computer time. As an alternative to this latter approach, the program also allows the operator to identify a few identical features on the two images prior to initiating the automated matching procedures.

Once the image pair is selected, the algorithm initiates one of two steps, depending upon the location of the area of interest. If the area is located within the central pack, area-based matching techniques are used to extract the ice motion, which is usually translational with only small rotations. In such cases several previous studies (Collins and Emery, 1988; Fily and Rothrock, 1986, 1987; Ninnis *et al.*, 1986; Vesecky *et al.*, 1988) have shown that the pack ice motion can be readily determined by finding the peak in the two-dimensional cross correlations of the intensity patterns on the two images. Included in this procedure is also a series of small image rotations to determine any rotational components of the motion. This procedure is carried out in two different stages, with the initial image matching occurring at a reduced resolution. The approximate translation vectors are then used to guide a higher resolution matching procedure, which determines the best match from the possible candidates.

To utilize this procedure in sea ice regions where large floe rotations occur requires a large computational effort. In such areas an initial extraction of distinct image features is carried out to increase the probability of finding successful matches. These regions are identified by the use of an iterative global clustering procedure that identifies the centroid of each cluster. The segmented regions can be areas of different ice types or of open water and are separated by boundaries. Once segmentation is completed, the boundaries between the regions are vectorized into one-dimensional data structures consisting of ordered pairs of numbers that represent the coordinates of the boundaries. These coordinate pairs are then transformed into a rotationally invariant curvilinear representation referred to a (Ψ,s) curve (Ballard and Brown, 1982), a process that replaces a computationally intensive 2-D process with the rapid 1-D matching of the (Ψ,s) segments using the normalized correlation as the similarity measure. In addition, the relative rotation of the features can be obtained, thereby providing valuable additional data. However, because the motion field generated by the feature matcher is localized at the feature boundaries, the coverage across an image is irregular. Therefore it is necessary to follow the application of the feature matching routine with an area-based matching technique that permits one to sample the motion field on a uniformly spaced grid. In this step fast Fourier transforms are utilized to obtain a more efficient registration of the translated and rotated image. The design also includes two different filtering processes and consistency checks. For instance, a match is classified as false if there are no local matches that support the hypothesis that its estimated motion is correct. Figure 3 illustrates the flow of the combined feature-based and area-based algorithms. Further discussion of a variety of facets of the (Ψ, s) matching procedures can be found in Kwok *et al.* (1990).

The ice motion data, consisting of a translation vector and an associated rotation angle describing the rotation of the image patch, will be sampled on the Special Sensor Microwave Imager (SSM/I) grid with a spacing of between 3 and 5 km. The absolute accuracy of the individual grid points is

estimated to be approximately 100 m for the ERS-1 SAR products. The selection of the SSM/I fixed-earth grid was made to simplify image coregistration, the analysis of kinematic data, the spatial mosaicing of motion data and comparisons with passive microwave measurements obtained from the SSM/I system. As is the case with all the data products of the GPS, once the analysis is completed, the data will be sent to the ASF Archive and Operations System (AOS) for distribution to the appropriate users and for storage. An example of three Seasat SAR images as well as the resulting output of the GPS Ice Motion Tracker is given in Figure 4.

Ice Classification: Although the development of a classifier that automatically determines the relative areal amounts of a specified number of ice types would appear to be simpler than tracking the sequential motions of drifting ice floes, at the present time it is the more difficult of the two tasks. This is particularly true if the classification procedure is required to distinguish between a useful selection of ice types and to be reliable during all the seasons of the year. The problem, of course, is that not only is the amount of C-band, VV polarized, 23° look angle, scatterometry data that adequately simulates the data from ERS-1 less than desired, but also some ice types of interest do not appear to have clearly separable backscatter values. As with the ice floe tracker, the input to the model will be the low resolution (100 m pixel spacing), 1024 × 1024 pixel images, although the processing of higher resolution images is possible.

The algorithm currently under development (Holt *et al.*, 1990a), which classifies returns into five different ice types (open water, new/young ice and first-year smooth, first-year rough and multiyear ice), is only believed to be reliable for winter ice conditions. The backscatter coefficient for open water shows large variations with sea state and is therefore a function of the wind speed and fetch. Therefore it can be very difficult to separate water from ice purely on the basis of the backscatter coefficient, and it may ultimately prove to be necessary to add textural measures or meteorological information to aid in this discrimination. In the above classification, new/young ice is a few centimetres thick and appears dark on SAR imagery, first-year smooth ice is less than a metre thick and is more inclined to raft than to ridge, while first-year rough ice is presumably in the thickness range of 1-2 m and shows the development of numerous pressure ridges. Multiyear ice is typically a few metres thick, has
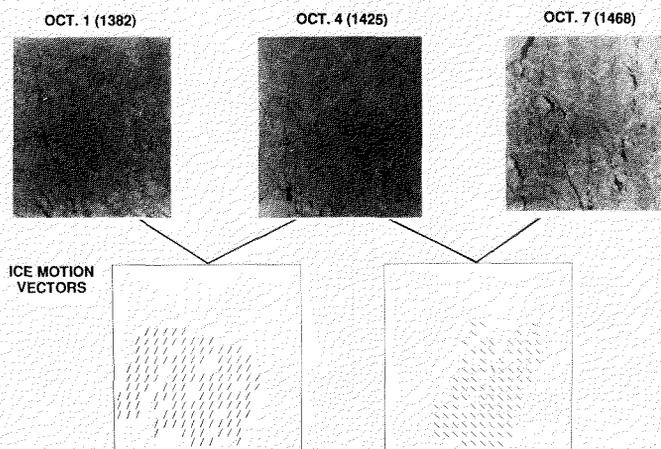
survived at least one summer and gives a strong radar return. Because multiyear ridges can be difficult to detect using C-band VV data, ridged and non-ridged multiyear ice are not considered as separate ice classes.

Figure 5 shows the flow chart for the GPS ice classification algorithm. As the initial step the program checks the meteorological information obtained from Unidata and tests to see if the air temperature is greater than −5°C at the field site at the time the SAR data was obtained. If so, it alerts the operator of this fact, as the algorithm is designed to function most accurately during the ice growth period from November to May. As the GPS is developed further, it is hoped that these seasonal restrictions can be removed by the development of additional look-up tables appropriate to specific regions and seasons. The algorithm then locates the corners of the image and masks out areas of land. It also determines whether the image lies near the ice edge or within an area of multiyear pack, based on digitizations of the National Oceanographic and Atmospheric Administration (NOAA) Ice Center's weekly ice maps.

The algorithm then selects the appropriate look-up table. As mentioned, at present there is only a table for winter conditions based on surface scatterometry data. Although these data suggest a clear separation between first-year and multiyear ice, the differences between first-year ice types are not particularly well resolved. In the classification images shown in Figure 6, the look-up table used was generated based on the images themselves. This procedure, which is also a possibility after launch, is not as *ad hoc* as it might seem in that ice observations from sequential imagery will provide considerable information on which signature corresponds to which ice type (e.g., ice that survives a summer is multiyear ice by definition).

A clustering routine is then used to perform an unsupervised segmentation of the data based on the number of clusters desired and their separation. The brightest class

FIG. 4. An example of the output from the GPS Ice Motion Tracker System based on Seasat SAR data obtained over a six-day period.
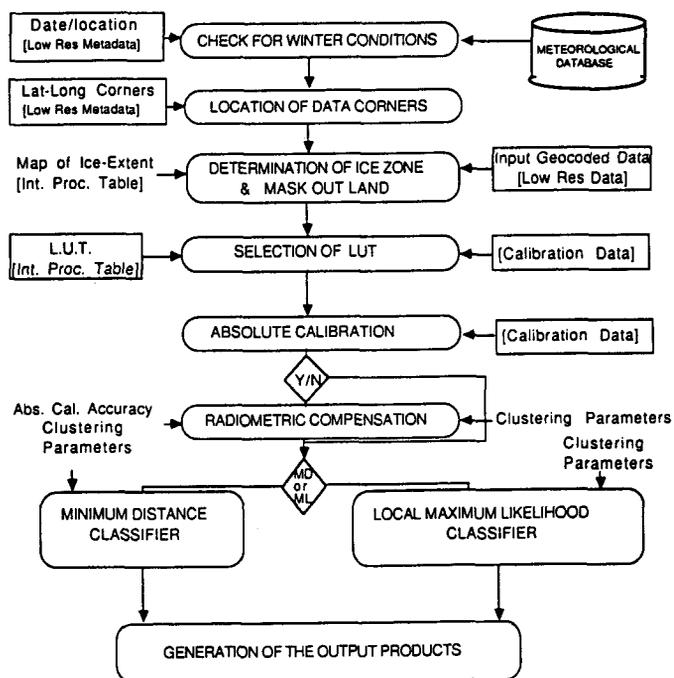

FIG. 5. The flow chart for the current version of the ice classification algorithm (Holt *et al.*, 1990a). (LUT = look-up table.)
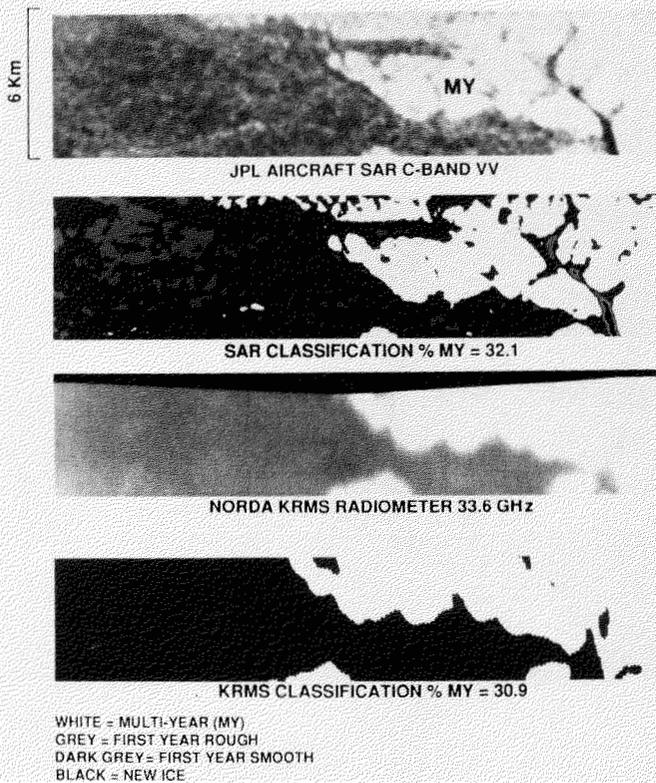
FIG. 6. An example of a GPS ice classification based on aircraft SAR data compared with a classification based on data from the KRMS 33.6 GHz radiometer (Holt *et al.*, 1990a).

is then compared to the largest mean in the look-up table. In cases where the NOAA ice charts indicate that multiyear ice is present in the sample, five clusters would be requested and the brightest cluster would be equated with the multiyear ice. In regions such as the Bering Sea, where multiyear ice does not occur, only four clusters would be requested and the initial match-up would be made with the first-year ice type with the largest backscatter. The other clusters are then assigned to the remaining ice classes based on their brightness level and separation. Following this, a series of radiometric corrections is made to produce a constant brightness level for multiyear ice (if present) across the image. Then the accuracy of the initial classification is enhanced by the use of either a minimum-distance classifier or a local-maximum-likelihood classifier (selectable by the operator). To date, comparisons of these two post-classifiers have resulted in estimates that differ by less than 2%. The output products, which are then transferred to the AOS for archiving and further distribution, are ice-type maps based on bins spaced at 5 km on the SSM/I grid and a map indicating the ice type for each pixel. Also included in the output will be the air temperature and wind speed. Needless to say, these procedures can undoubtedly be expanded and improved. This is a task that will receive considerable attention during the first year after ERS-1's launch. More detail on the ice classification algorithm can be found in Holt *et al.* (1989, 1990a).

Waves: There are two primary problems that must be considered in applying ERS-1 SAR data to ocean wave problems. First, there is still considerable controversy over the exact mechanisms of wave imaging. Nevertheless, considerable useful information can be collected despite the lack of agreement on mechanistic details. Recent studies have shown

that the unmodified SAR spectrum provides good estimates of peak directional wavelengths and wave directions when comparisons are made with buoy observations (Napolitano *et al.*, 1989). In an attempt to skirt this debate about imaging mechanisms, a product will be provided that makes verifiable estimates of wave properties and that can be used later, if necessary, as a component in more sophisticated treatments. Second, significant non-linearities can develop in the measurement of waves that are traveling parallel to the direction of the satellite as the result of the presumed random Doppler motion of the ocean scatterers during the SAR integration time; this process is enhanced by steep waves and increased satellite height. In the following the problem of non-linear behavior in the SAR imaging of waves is "treated" by having the program raise a flag that alerts users when the waves considered are traveling within 30° of the satellite direction.

The wave algorithm, which is comparatively straightforward relative to the two previous algorithms, is used only on request and utilizes up to 24 subscenes (512 × 512 pixels each) of a full 30 m resolution (12.5 m pixel spacing), 4-look-format image that has been corrected to the ground range format. After automatically querying the AOS to locate the full resolution image and extract the requested subscenes, the algorithm performs a 2-D fast Fourier transform on each subscene, applies a smoothing filter to remove the image mean and utilizes a peak finding routine to locate the wave peaks in the smoothed spectra. The wavelength is then determined by the peak distance from the origin in wave number space and the wave direction by the orientation of the peaks from the origin. The final output of the program is a contoured plot of the wave spectra. Examples of several spectra obtained of waves moving through the marginal sea ice zone in the Chukchi Sea are shown in Figure 7. For a more detailed description of the wave algorithm, the reader is referred to Holt *et al.* (1990b). It should be noted that after the launch of ERS-1 verification of the adequacy of the above procedures will be obtained through comparisons with wave buoy data. The positions of several NOAA environmental buoys that obtain omnidirectional wave spectra and that are located within the station mask are shown in Figure 2.

FUTURE PRODUCTS

Although the present set of GPS products will be a significant step forward, it clearly would be misleading to claim that everything is presently in order. For example, even if we are ultimately able to unambiguously separate ice from open water and to classify sea ice into several different ice types, we still do not have the information we need. What is really needed is a SAR analysis system that at the end of each summer notes the presence of the surviving ice, labels it as multiyear and keeps track of where it is located throughout the following year. In addition, the system must note when different areas of first-year ice form and keep track of their locations throughout the year. Each subsequent lead formation and freeze-over event would, in turn, initiate new ice areas whose thickness could be estimated by several different procedures of varying complexity, starting with simple degree-day calculations (Maykut, 1986). During compressional events the different ice thicknesses destroyed would also be noted and transferred to a ridged category.

Although this would appear to be a staggering bookkeeping job, in principle it can be done. As a first simplified step,
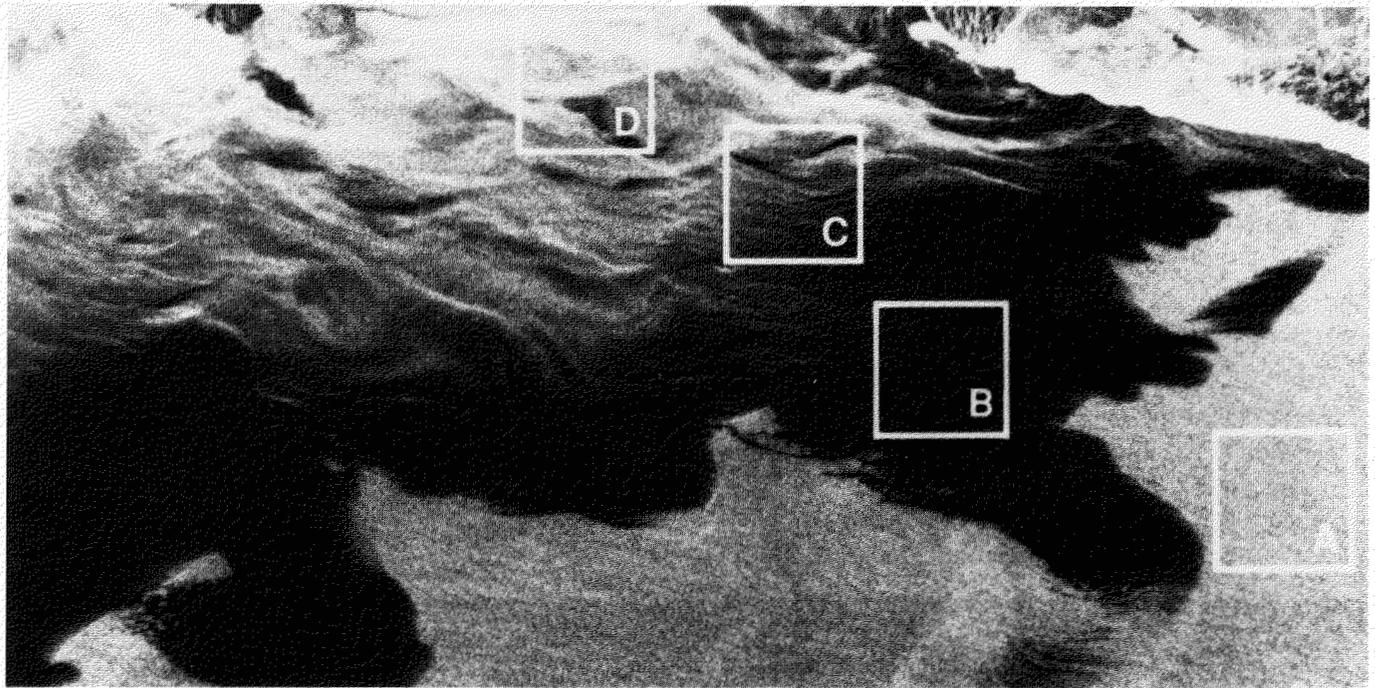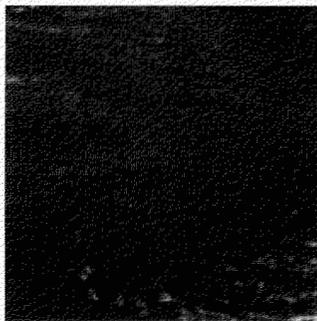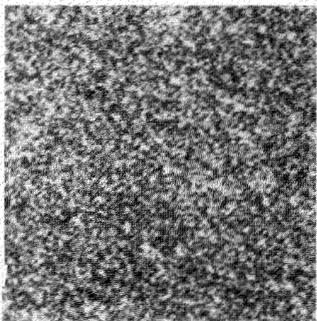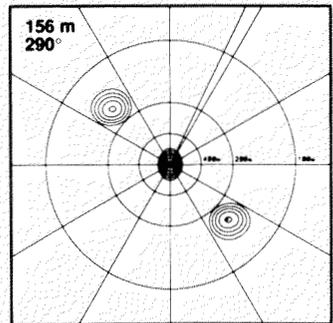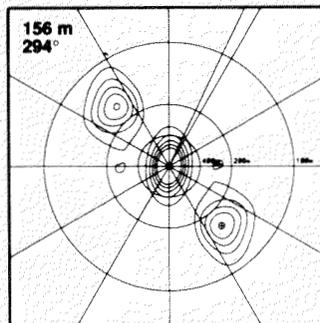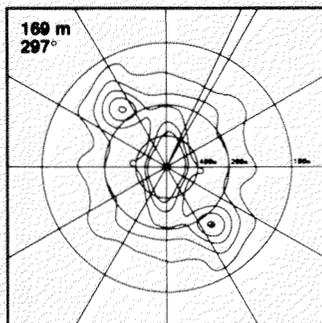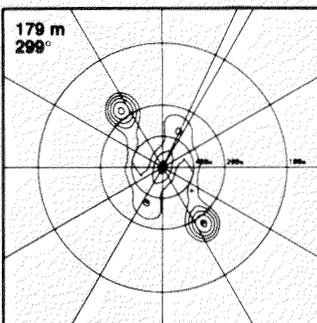
FIG. 7. Wave spectra plots shown with the associated Seasat SAR scene and subscenes for a region within the marginal sea ice zone of the Chukchi Sea (Holt et al., 1990b). The date of the imagery was 8 October 1978.

one would perhaps consider only four ice types: open water, first-year < 50 cm thick ice, first-year > 50 cm thick ice and multiyear ice. Assuming that a clear distinction could be made between open water and ice, ice growth would only be cal-culated until the estimated ice thickness exceeds 50 cm. The underlying physical basis for this distinction is, of course, the fact that ice < 50 cm thick and open water are the major contributors to the heat flux into the atmosphere and the

salt flux into the ocean (Maykut, 1986). Utilization of such a cutoff value would both focus attention on the more important thin ice areas and reduce the overall computational effort. It would also serve to eliminate the snow problem, because ice < 50 cm thick has usually not had enough time to develop a significant snow cover.

To date there has been only one study that has attempted to use digital SAR measurements to measure the opening and closing of leads (Fily and Rothrock, 1990). In the procedure used the displacements are determined automatically on a regular grid by cross-correlation. Then an algorithm groups together cells that cover a lead event and estimates the lead area change by counting lead pixels before and after deformation. Errors, which were estimated by comparison with area changes determined from manually digitized lead boundaries, were found to be about 0.2% of the area of the scene. It was observed that although large events were responsible for most of the deformation, the cumulative contribution of many small openings and closings was also important to the total. Another significant result is that if area changes are to be estimated to values on the order of 0.1% or less, as would appear to be geophysically desirable, very precise range corrections across images are essential. The results are also less than encouraging since the procedures used are not readily automated and the attempts to simplify the procedures in ways that might facilitate automation were not particularly successful.

Clearly this subject requires more study. If adequate automated procedures can be devised, the potential payoff in geophysical understanding will be very large. We note that such automation is not merely a nicety, considering that by the time of the launch of Radarsat in 1994, the capability will exist to obtain SAR imagery of the world's complete bipolar sea ice covers on a weekly basis. If the above can be accomplished, the capability currently exists to calculate not only the changes in thicknesses of the new ice formed as the result of lead formation, but the properties of the ice as well. For a review of current activities on that front and their implications for remote sensing, the reader is referred to papers by Cox and Weeks (1988) and by Maykut et al. (1991). Additional interesting comments on the analysis problems and opportunities that will be presented by the impending onslaught of SAR data can be found in Rothrock (1988).

Although here we have stressed polar ocean applications of SAR, it should be noted that ASF science planning (ASFPSWT, 1989) anticipates that SAR data will contribute to a wide variety of studies in the fields of glaciology, structural and quaternary geology, volcanology, hydrology, ecosystem studies and remote sensing science. In the broadest sense, the ASF program will contribute to studies of changes in the polar regions in which differences in either the surface roughness or the dielectric properties of the earth's surface layer are important.

ACKNOWLEDGEMENTS

REFERENCES

APEL, J.R., and GONZALEZ, F.I. 1983. Nonlinear features of internal waves off Baja California as observed from the Seasat imaging radar. Journal of Geophysical Research 88(C7):4459-4466.

ASFPSWT (Alaska SAR Facility Prelaunch Science Working Team). 1989. Science Plan for the Alaska SAR Facility Program, Phase 1: Data from the First European Remote Sensing Satellite, ERS-1. Jet Propulsion Laboratory JPL Publication 89-14:1-87.

BADGLEY, F.I. 1966. Heat budget at the surface of the Arctic Ocean. In: Proceedings of the Symposium on the Arctic Heat Budget and Atmospheric Circulation. RM-5233-NSF. Santa Monica, California: The RAND Corporation. 267-278.

BALLARD, D.H., and BROWN, C. M. 1982. Computer Vision. Englewood Cliffs, New Jersey: Prentice-Hall.

CARSEY, F.D., and HOLT, B. 1987. Beaufort-Chukchi ice margin data from Seasat: Ice motion. Journal of Geophysical Research 92(C7):7163-7172.

COLLINS, M.J., and EMERY, W.J. 1988. A computational method for estimating sea ice motion in sequential Seasat synthetic aperture imagery by matched filtering. Journal of Geophysical Research 93(C8):9241-9251.

COLONY, R., and THORNDIKE, A.S. 1984. An estimate of the mean field of arctic sea ice motion. Journal of Geophysical Research 89(C8):10623-10629.

COX, G.F.N., and WEEKS, W.F. 1988. Numerical simulations of the profile properties of undeformed first-year sea ice during the growth season. Journal of Geophysical Research 93(C10):12449-12460.

CURLANDER, J.C., HOLT, B., and HUSSEY, K.J. 1985. Determination of sea ice motion using digital SAR imagery. Institute of Electrical and Electronic Engineers Journal of Oceanic Engineering OE-10(4):358-367.

FILY, M., and ROTHROCK, D.A. 1986. Extracting sea ice data from satellite SAR imagery. Institute of Electrical and Electronic Engineers Transactions on Geoscience and Remote Sensing GE-24(6):849-854.

FILY, M., and ROTHROCK, D.A. 1987. Sea ice tracking by nested correlations. Institute of Electrical and Electronic Engineers Transactions on Geoscience and Remote Sensing GE-25(5):570-580.

FILY, M., and ROTHROCK, D.A. 1990. Opening and closing of sea ice leads: Digital measurements from SAR. Journal of Geophysical Research 95(C1):789-796.

FU, L.-L., and HOLT, B. 1983. Seasat views oceans and sea ice with Synthetic Aperture Radar. JPL Publication 81-120. Pasadena, California: Jet Propulsion Laboratory.

FU, L.-L., and HOLT, B. 1984. Internal waves in the Gulf of California: Observations from a spaceborne radar. Journal of Geophysical Research 89(C2):2053-2060.

HALL, R.T., and ROTHROCK, D.A. 1981. Sea-ice displacements from Seasat synthetic aperture radar. Journal of Geophysical Research 86(C11):11078-11082.

HOLT, B., KWOK, R., and RIGNOT, E. 1989. Ice classification algorithm development and verification for the Alaska SAR Facility using aircraft imagery. International Geoscience And Remote Sensing Symposium (IGARSS'89) 2:751-754.

HOLT, B., KWOK, R., and RIGNOT, E. 1990a. Status of the ice classification algorithm in the Alaska SAR Facility Geophysical Processor System. International Geoscience And Remote Sensing Symposium (IGARSS'90):2221-2224.

HOLT, B., KWOK, R., and SHIMADA, J. 1990b. Ocean wave products from the Alaska SAR Facility Geophysical Processor System. International Geoscience And Remote Sensing Symposium (IGARSS'90):1469-1472.

KWOK, R., CURLANDER, J.C., McCONNELL, R., and PANG, S.S. 1990. An ice motion tracking system at the Alaska SAR Facility. Institute of Electrical and Electronic Engineers Journal of Oceanic Engineering 15(1):44-54.

LEBERL, F., RAGGAM, J., ELACHI, C., and CAMPBELL, W.J. 1983. Sea-ice measurements from Seasat SAR images. Journal of Geophysical Research 88(C3):1915-1928.

MANABE, S., and STOUFFER, R.J. 1980. Sensitivity of a global climate model to an increase of CO_2 concentration in the atmosphere. Journal of Geophysical Research 85(C10):5529-5554.

MAYKUT, G.A. 1986. The surface heat and mass balance. In: Untersteiner, N., ed. The Geophysics of Sea Ice. Vol. 146. New York: Plenum Press. 395-463.

MAYKUT, G.A., GRENFELL, T.C., and WEEKS, W.F. 1991. On estimating spatial and temporal variations in the properties of ice in the polar oceans. In: Nihoul, J., ed. 22nd International Liege Symposium on Ice Covered Seas and Ice Edges; physical, chemical and biological processes and interactions, Liege, Belgium. Journal of Marine Systems. In press.

MUENCH, R.D., MARTIN, S., and OVERLAND, J.E. 1987. Preface to the special issue on the Marginal Ice Zone. Journal of Geophysical Research 92(C7):6715-6716.

NAPOLITANO, D.J., VESECKY, J.F., GONZALEZ, F., and PETE-HERYCH, S. 1989. SAR measurements of ocean waves and other phenomena during the GOASEX Experiment. International Geoscience And Remote Sensing Symposium (IGARSS'89) 4:2331-2334.

NINNIS, R.M., EMERY, W.J., and COLLINS, M.J. 1986. Automated extraction of pack ice motion from Advanced Very High Resolution imagery. Journal of Geophysical Research 91(C9):10725-10734.

PEASE, C.H., and OVERLAND, J.E. 1984. An atmospherically driven sea-ice drift model for the Bering Sea. Annals of Glaciology 5:111-114.

ROTHROCK, D.A. 1988. Automated ice measurements from a decade of SAR imagery — How will we get them? How will we use them? In: Workshop on Instrumentation and Measurements in the Polar Regions, Monterey, California 27-29 January 1988, Marine Technology Society. 35-44.

ROYER, T.C., and MUENCH, R.D. 1977. On the temperature distribution in the Gulf of Alaska. Journal of Physical Oceanography 7:92-99.

SERREZE, M.C., BARRY, R.G., and McLAREN, A.S. 1989. Seasonal variations in sea ice motion and effects on sea ice concentration in the Canada Basin. Journal of Geophysical Research 94(C8):10955-10970.

SIR-C. 1986. Shuttle Imaging Radar-C Science Plan. Jet Propulsion Laboratory JPL Publication 86-29:1-178.

THORNDIKE, A.S., and COLONY, R. 1982. Sea ice motion in response to geostrophic winds. Journal of Geophysical Research 87(C8):5845-5852.

VESECKY, J.F., SAMADANI, R., SMITH, M.P., DAIDA, J., and BRACEWELL, R. 1988. Observations of sea-ice dynamics using synthetic aperture radar images: Automated analysis. Institute of Electrical and Electronic Engineers Transactions on Geoscience and Remote Sensing GE-26(1):38-47.

WEEKS, W.F., KOVACS, A., and HIBLER, W.D., III. 1971. Pressure ridge characteristics in the arctic coastal environment. In: Proceedings First International Conference on Port and Ocean Engineering under Arctic Conditions (POAC'71). Vol. I. Trondheim: The Technical University of Norway. 152-183.

WEEKS, W.F., GOW, A.J., and SCHERTLER, R.J. 1981. Ground-truth observations of ice-covered North Slope lakes imaged by radar. Report 81-19. Hanover, New Hampshire: Cold Regions Research and Engineering Laboratory. 1-17.